Apoptosis of lung carcinoma cells induced by a flexible optical fiber-based cold microplasma

Jae Young Kim [a], John Ballato [b], Paul Foy [b], Thomas Hawkins [b], Yanzhang Wei [c], Jinhua Li [c], Sung-O. Kim [a,*]

[a] Holcombe Department of Electrical and Computer Engineering, Center for Optical Materials Science and Engineering Technologies (COMSET), Clemson University, Clemson, SC 29634, USA
[b] School of Material Science and Engineering, Center for Optical Materials Science and Engineering Technologies (COMSET), Clemson University, Clemson, SC, 29634, USA
[c] Department of Biological Sciences, Clemson University Biomedical Institute, Clemson University, Greenville, SC 29605, USA

ABSTRACT

Atmospheric pressure plasmas have been used as a therapy for cancer. However, the fairly large size and rigidity of present plasma-delivery systems obstructs the precise treatment of tumors in harder-to-reach internal organs such as the lungs, pancreas, and duodenum. In order to improve the targeted delivery of plasmas a highly flexible microplasma jet device is fabricated using a hollow-core optical fiber with an inner diameter of either 15 μm, 55 μm, or 200 μm. Described herein, based on this device, are results on lung carcinoma therapy using a microplasma cancer endoscope. Despite the small inner diameter and the low gas flow rate, the generated plasma jets are shown to be sufficiently effective to induce apoptosis, but not necrosis, in both cultured mouse lung carcinoma and fibroblast cells. Further, the lung carcinoma cells were found to be more sensitive to plasma treatment than the fibroblast cells based on the overall plasma dose conditions. This work enables directed cancer therapies using on highly flexible and precise hollow optical fiber-based plasma device and offers enhancements to microplasma cancer endoscopy using an improved method of plasma targeting and delivery.

© 2011 Elsevier B.V. All rights reserved.

1. Introduction

A plasma is an ionized medium that contains numerous active components including electrons and ions, free radicals, reactive molecules, and photons (Becker et al., 2006; Cooper et al., 2009; Kushner, 2005; Laroussi and Lu, 2005; Somekawa et al., 2005). Plasma treatment has been used for materials processing in order to impart desired surface characteristics on plastics, paper, textiles, semiconductors (Kim et al., 2006; Noeske et al., 2004; Temmerman et al., 2005; Yang and Yin, 2007). The demonstration of atmospheric plasma processes broadened the field to include treatment of materials that generally are unsuitable for vacuum processes. Such improvements in the state-of-the-art have led to the emergence of biological applications for plasmas. Plasmas can be categorized as either thermal (hot) or non-thermal (cold) (Tendero et al., 2006). In a thermal plasma, the electrons and heavy particles are in equilibrium with one another and the environment and the temperature of the heavy particles is nearly equal to that of the electrons. On the other hand, a non-thermal plasma shows very high electron temperatures but low gas temperatures due to a weak ionization rate. Due to the large difference in mass, the electrons come into ther-

modynamic equilibrium among themselves much faster than they come into the equilibrium with the heavy particles, such as ions and neutral atoms. As a result, the overall temperature of the plasma can remain much cooler than the electron temperature, nearly the ambient temperature. Atmospheric non-thermal plasma treatments are being investigated for multiple biological applications including tissue sterilization, blood coagulation, wound healing, tissue regeneration, dental treatment, and the treatment of various diseases, including cancer (Fridman et al., 2008; Kong et al., 2009; Kim et al., 2010a,b; Lee et al., 2010; Morfill et al., 2009; Scholtz et al., 2010). The plasma cancer therapies that have been developed utilize excited radicals, including reactive oxygen species (ROS), and directly expose these to the tumor cells at macro-scale dimensions such that apoptosis is induced at a rapid pace (Fridman et al., 2008; Georgescu and Lupu, 2010; Kim et al., 2010b; Stoffels et al., 2008). However, present devices are macro-sized and generally more rigid thus limiting the precise targeting of plasma treatment in internal organs.

Lung cancer is one of the most common cancers in North America for both men and women and is a leading cause of cancer-related deaths (Jemal et al., 2010) because the majority of lung cancers are inoperable. In order to better treat lung cancer using a non-thermal plasma, a plasma jet device should be flexible and small in diameter so that a well-defined plasma can be delivered to a specific biological site in the body. A hollow-core optical fiber serving as

an effective conduit for a delivery of atmospheric pressure plasma has several advantages including excellent flexibility, very small diameter, mechanical robustness, chemical durability, and very low production cost. The flexible and micrometer-scale plasma jet devices with a hollow-core optical fiber could be utilized to access internal sites through minimally-invasive surgical procedures similar to an endoscopic within internal organs including the lungs. In addition, the flexible microplasma jet devices employing a hollow-core optical fiber with a low gas flow rate can prevent unwanted blood coagulations during the plasma treatment of tumor cells unlike the present plasma devices.

In this paper, a highly flexible microplasma jet device is developed using hollow-core optical fibers and their use in targeted cancer treatment therapies is investigated. This work permits new directed cancer therapies based on a highly flexible and precisely-positioned hollow optical fiber-based microplasma jet device and offers microplasma cancer endoscopy as a new physical cancer therapeutic method.

2. Materials and methods

2.1. Hollow-core optical fiber as a conduit for plasmas

A series of hollow glass optical fibers with inner diameters of 15 μm, 55 μm, and 200 μm, respectively, were fabricated at Clemson University using a custom-designed commercial-scale Heathway optical fiber draw tower. Regarding the hollow glass fiber with the inner diameter of 15 μm, a fused silica tube (Heraeus Tenevo, Buford GA) with inner diameter of 8 mm and outer diameter of 26 mm was drawn at a temperature of approximately 1895 °C and rate of approximately 12 m/min. Regarding the hollow glass fiber with the inner diameter of 55 μm, a fused silica tube with inner diameter of 13 mm and outer diameter of 26 mm was drawn at a temperature of approximately 1930 °C and rate of approximately 16 m/min. Regarding the hollow glass fiber with the inner diameter of 200 μm, a fused silica tube with inner diameter of about 7 mm and outer diameter of about 10 mm was drawn at a temperature of approximately 1915 °C and rate of approximately 5.5 m/min.

2.2. Fabrication of the hollow-core optical fiber-based plasma jet devices

Developed for use in this work was a flexible microplasma jet device comprising hollow-core optical fibers of three different sizes. A basic microplasma jet device has a very simple structure consisting of a tube with electrodes. The devices have a single electrode configuration, which was placed a certain distance from the end of the optical fiber in order to generate the direct plasma mode

(Fridman et al., 2007; Jiang et al., 2009; Kim et al., 2010c). In direct plasma mode, since the plasma plume itself contacts the treated surface, both charged species and a significant electric flux reach the treatment area (Fridman et al., 2007). In order to generate a stable plasma plume, the microplasma device design and driving conditions (e.g., applied voltage and gas flow) were experimentally optimized, with detailed specifications on the three flexible microplasma jet devices being listed in Table 1. As is shown in Fig. 1A, the plasma plume from these highly flexible microplasma jet devices would be able to precisely target a small collection of cells.

2.3. System for atmospheric pressure microplasma jets

A whole system of atmospheric pressure microplasma jet devices is described in Fig. 1B. The voltage and current waveforms from the single electrode were measured using a high voltage probe (Tektronix P6015A) and a current probe (Pearson current monitor 4100) in order to monitor power consumption. In the driving circuit, an inverter was used to amplify a low primary voltage to a high secondary voltage. A sinusoidal voltage, with a peak value of several kilovolts and a fixed frequency of 32 kHz was applied to the single electrode of the microplasma devices. High purity helium gas was used as the carrier gas. Helium gas promotes chemical safety given its inertness and can yield plasmas at lower input voltages than other gases (Kieft et al., 2004). The helium gas flow rates were 10 standard cubic centimeters per minute (sccm), 35 sccm, and 100 sccm for the hollow optical fibers of 15 μm, 55 μm, and 200 μm inner diameters, respectively. Compared to previous plasma jet devices with millimeter-sized tubes (1000–40,000 sccm), these gas flows are remarkably low (Feng et al., 2010; Hong and Uhm, 2007; Karakas et al., 2010; Kim et al., 2008, 2009; Lu et al., 2008; Nie et al., 2008; Nikiforov et al., 2011; Rupf et al., 2010; Sands et al., 2008; Shashurin et al., 2008; Walsh and Kong, 2008). Another benefit of these small diameter devices is that the low gas flow rates reduce the dehydration of cells (Kieft et al., 2006).

2.4. Cell preparation and cell treatments by microplasma jets for Annexin V-FITC assay

For the Annexin V-FITC assay, TC-1 mouse lung carcinoma cells (ATCC No. JHU-1) and mouse fibroblast CL.7 cells (ATCC TIB-80) were seeded in wells of 24-well plates (2×10^5 cell/well) in duplication and cultured in DMEM (Gibco BRL, Grand Island, NY), supplemented with 10% FBS (Hyclone, Logan, UT) and 50 μg/ml gentamicin (Gibco BRL) at 37 °C in a humidified atmosphere of 5% CO_2 for 24 h. Prior to plasma treatment, the cells at approximately 90% confluence were washed twice with PBS and treated with plasmas. After plasma treatments, the wells were imme-

Table 1
Specifications of three flexible microplasma jet devices, Device I, II, and III, utilizing hollow-core optical fibers of 15 μm, 55 μm, and 200 μm inner diameters, respectively.

Specifications		Device I	Device II	Device III
Hollow optical fiber	Inner diameter (I.D.)	15 μm	55 μm	200 μm
	Outer diameter (O.D.)	60 μm	125 μm	300 μm
	Full diameter	125 μm	240 μm	440 μm
Electrode	Material	Silver paste	Copper tape	Copper tape
	Distance from orifice	1 mm	5 mm	10 mm
	Width	6 mm	6 mm	6 mm
Gas condition	Carrier gas	Helium	Helium	Helium
	Gas flow rate	10 sccm	35 sccm	100 sccm
	Linear gas velocity[a]	943 m/s	246 m/s	53.1 m/s
Driving condition	Applied voltage (V_p)	9 kV	7.5 kV	6 kV
	Frequency	32 kHz	32 kHz	32 kHz
	Power consumption[b]	34.7 W	23.5 W	15.5 W

[a] The linear gas velocity is calculated using the inner diameter and gas flow rate.
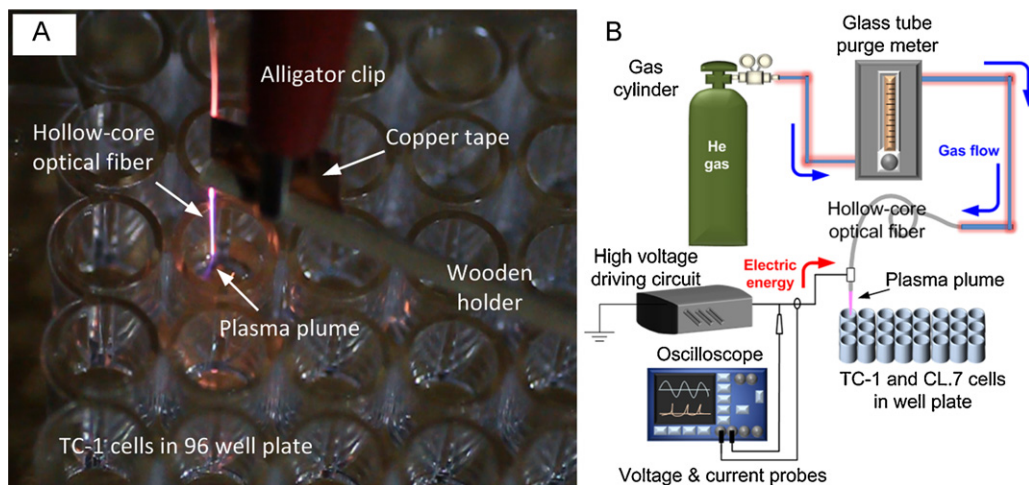[b] The power consumption is calculated as $P = I_{rms} \times V_{rms}$.

Fig. 1. Flexible microplasma jet device based on a hollow-core glass optical fiber. (A) Photograph of plasma plume from the hollow-core optical fiber (55 μm inner diameter) and cell treatments on a 96 well plate. (B) Schematic diagram of microplasma jet system.

diately filled with cell culture medium and incubated for 24 h. After harvesting and washing twice with PBS, the cells, including adherent and non-adherent cells, were analyzed for apoptosis using the Annexin V-FITC Apoptosis Detection Kit (eBiosciences, www.ebiosciences.com) and a FACS Calibur (BD Biosciences, San Jose, CA).

2.5. Cell preparation and cell treatments by microplasma jets for TUNEL assay

For the TUNEL assay, TC-1 tumor cells and CL.7 fibroblast cells were seeded into wells of 96-well flat bottom plates (3×10^4 cell/well) in duplication. After 24 h, the culture media were removed from the wells and the cells were treated only once with three plasma jets for 20 s. The apoptotic responses were identified in the well Plate 24 h later using Invitrogen's Click-iT® TUNEL Alexa Fluor® 488 Imaging Assay kit according to the manufacturer's protocol.

3. Results and discussion

3.1. Plasma plumes from hollow-core optical fiber based plasma jet devices

The hollow-core optical fibers consist of a glass capillary that is externally coated with a protective plastic coating. The images provided in Fig. 2A–C, shows a close comparison of the dimensions of TC-1 mouse lung carcinoma cells and the hollow-core optical fiber with an inner (hollow) diameter of 15 μm, 55 μm, and 200 μm, respectively. Since the plasma is confined inside the hollow glass fiber, the inner diameter determines the plasma plume width. The total diameter of the fiber determines the flexibility and degree to which the plasma can be delivered to a desired biological site within the body. It is important to note that electrons cannot be sufficiently accelerated and, accordingly, the electron energy is not sufficient to ionize the neutral gases when the discharge volume became smaller, resulting in failure of discharge (Becker et al., 2006). Thus, much higher electrical energies are required to initiate and sustain the plasma discharge in smaller fiber volumes (i.e., smaller hollow core diameters). Therefore, even though the three microplasma jet devices are basically the same structure, consisting of a glass tube, in which gas flows, and a single electrode, each device has different discharge conditions due to the different plasma volume as deter-

mined by an inner diameter of the fiber. The discharge condition for each of the three flexible microplasma jet devices also is summarized in Table 1. When sinusoidal voltages, with peak values of 9 kV, 7.5 kV, and 6 kV, respectively, and a fixed frequency of 32 kHz are applied to the electrodes of the three microplasma devices, the corresponding plasma plumes are about 5 mm in length, as is shown in Fig. 2D–F. The plasma plumes in ambient air are sufficiently long to provide direct treatment to a small collection of tumor cells.

3.2. Apoptotic analysis of microplasma treatments using Annexin V-FITC

Using these three devices, microplasma jets were applied to both mouse TC-1 lung carcinoma and CL.7 fibroblast cells in order to study the influence of the plasma treatment. Fig. 3 shows the apoptotic results of the plasma treatments with a flow cytometric analysis on the TC-1 lung carcinoma cells and the CL.7 fibroblast cells at doses of 0 s (no treatment), 2 s, 5 s, and 10 s, respectively. In each well, 6 spots were treated clockwise, with the distance between the plasma jet devices and the cells being about 5 mm. The upper graphs in Fig. 3 show the increased rates in apoptosis of cells based on the Annexin V-FITC in mouse TC-1 lung carcinoma cells. The lower graphs represent the same in murine CL.7 fibroblast cells. The raw data from Annexin V-FITC methods are provided in Figs. S1–3 in Supplementary Data.

Under these experimental conditions, despite the small size of the plasma plume and low gas flow rate, the plasmas yielded practical results for the induction of dose-dependent apoptosis in the cultured cells. The plasma did not affect a necrotic response under all experimental conditions. Interestingly, although Device I (15 μm-sized flexible microplasma device) had the highest voltage and power consumption (Table 1), it induced the least apoptotic response in both TC-1 and CL.7 cells. In contrast, Device III (200 μm-sized flexible microplasma device), which had the lowest voltage and power consumption induced the biggest apoptotic response in both cells. Since the plasma plume is confined in the inner diameter of the fiber, a larger sized microplasma device has a wider plasma plume and, therefore, treats a larger area. The comparison of the three microplasma jet devices used in this work revealed that the plasma size is a more dominant factor in the induction of an apoptotic response in the cells than the plasma driving condition when the same carrier gas is used.
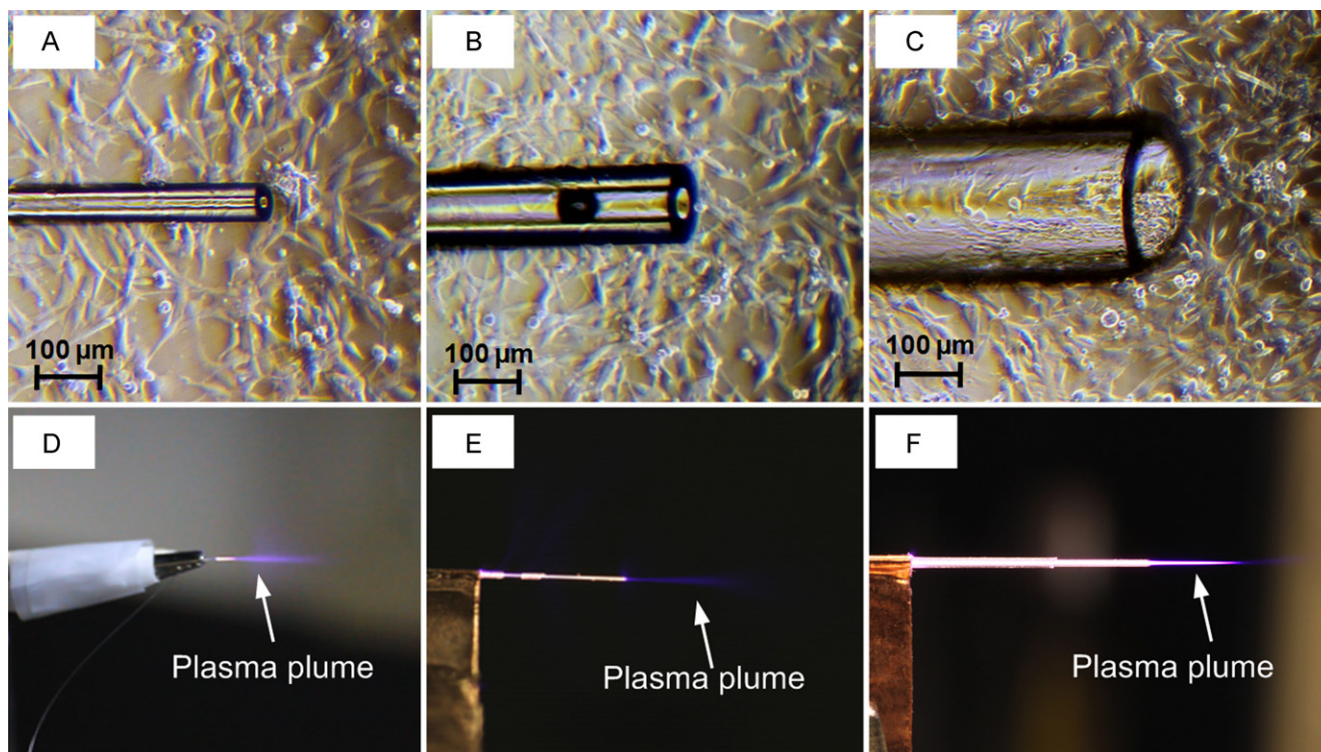
Fig. 2. Three flexible microplasma jet devices employed in this study. Dimensional comparisons between TC-1 mouse lung carcinoma cells and the hollow-core optical fibers with inner diameters of (A) 15 μm, (B) 55 μm, and (C) 200 μm, respectively. Photographs of plasma plume from (D) Device I (15 μm-sized microplasma jet), (E) Device II (55 μm-sized microplasma jet), and (F) Device III (200 μm-sized microplasma jet) into the ambient air, respectively.

The proportion of apoptotic live and apoptotic dead TC-1 tumor cells treated with plasmas is higher than that of fibroblast CL.7 cells at dose durations of 2 s, 5 s, and 10 s under all experimental conditions, as is shown in Fig. 3. The proportion of apoptotic live and apoptotic dead TC-1 tumor cells treated with plasma (6 times at 10 s doses) are approximately 4.5 times (23.2% vs. 4.92%), 2.5 times (23.59% vs. 9.49%), and 1.5 times (28.11% vs. 18.97%) greater than CL.7 cells treated with same plasma dosages treated by Device I
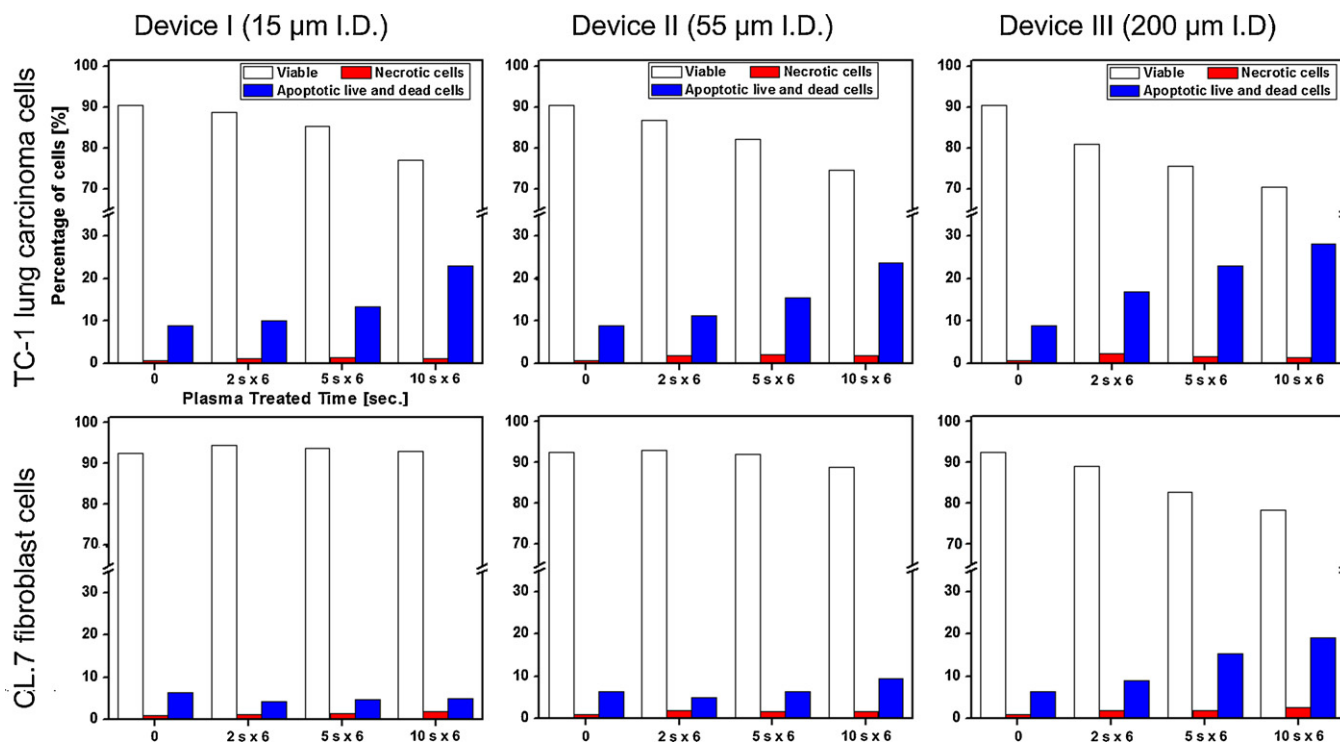

Fig. 3. Apoptotic analysis using the Annexin V-FITC in TC-1 mouse lung carcinoma cells (top row of figure) and fibroblast CL.7 cells (bottom row of figure). Plasma treatments by three microplasma jets (Device I, II, and III) were performed on either mouse lung carcinoma TC-1 cells or fibroblast CL.7 cells at doses of 0 s (no treatment), 2 s × 6, 5 s × 6, and 10 s × 6, respectively. The graphs represent the percentage of the cells in the region among the total number of cells.
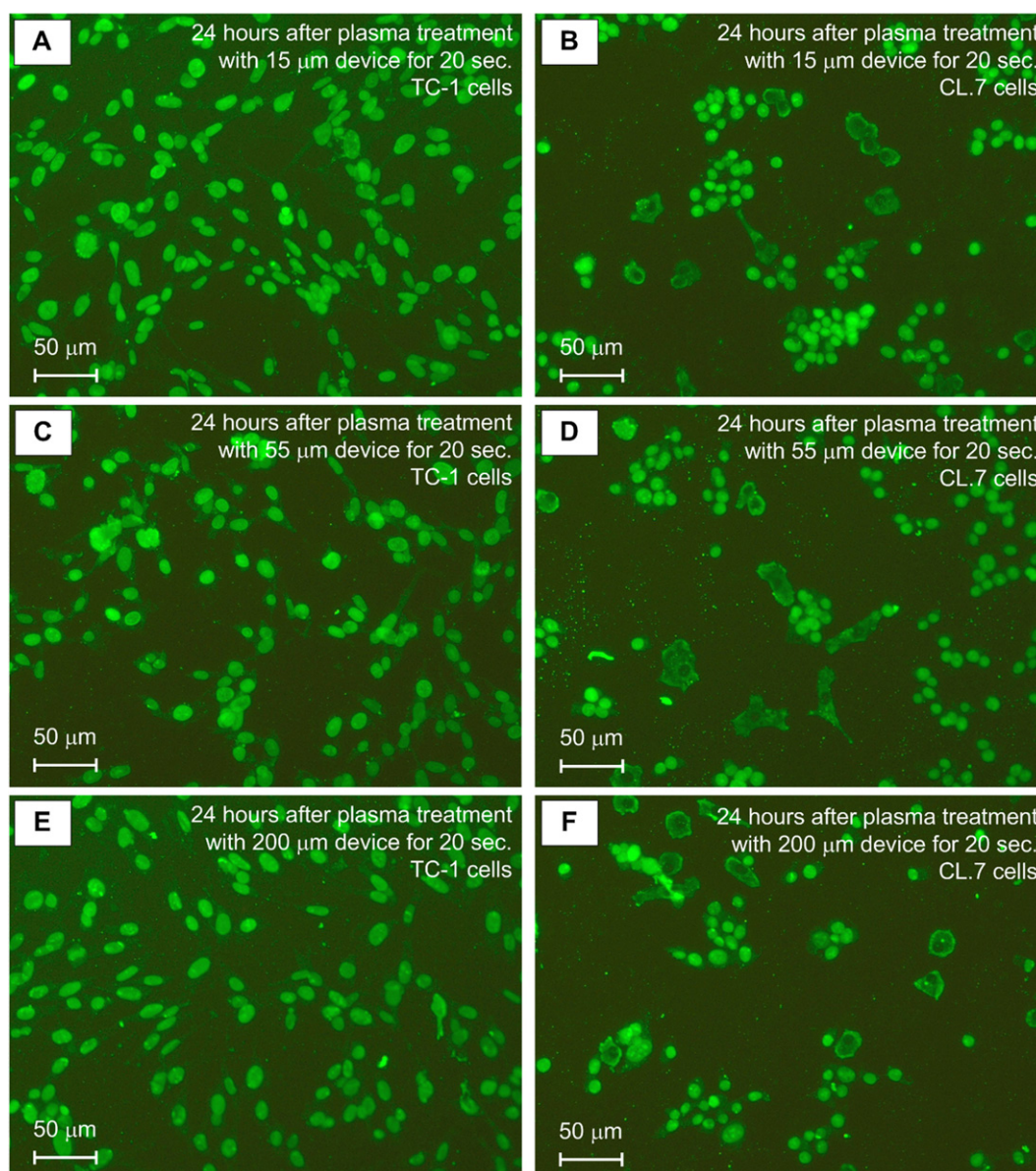
Fig. 4. Apoptotic responses using TUNEL assay kit in TC-1 cells and CL.7 cells treated by Device I, II, and III; (A) TC-1 cells and (B) CL.7 cells treated by Device I. (C) TC-1 cells and (D) CL.7 cells treated by Device II. (E) TC-1 cells and (F) CL.7 cells treated by Device III. Twenty-four hours after plasma treatment of cultured murine cells for 20 s, in the TC-1 cells, most cells are dyed within the plasma treated area. However, in the CL.7 cells, both dyed and un-dyed cells are mixed within the plasma treated area. TC-1 and CL.7 cells treated by the three microplasma jets are the almost same in appearance following identical plasma treatment times of 20 s.

(15 μm-sized hollow optical fiber), Device II (55 μm-sized hollow optical fiber), and Device III (200 μm-sized hollow optical fiber), respectively. (see Fig. 3 and Figs. S1–3 in Supplementary Data). This shows that the TC-1 tumor cells are more sensitive to plasma treatment than CL.7 fibroblast cells under these experimental conditions. Strikingly, at dose duration of 2 s, 5 s, and 10 s in the case of Device I and at dose duration of 2 s and 5 s in the case of Device II, the microplasmas induced the TC-1 tumor cells to undergo apoptosis, but not the CL.7 fibroblast cells. These results indicate that microplasmas can be used to selectively terminate TC-1 tumor cells with no harm to CL.7 fibroblast cells under these plasma dose conditions.

3.3. Apoptotic analysis of microplasma treatments using TUNEL assay

The induction of apoptosis in cultured murine tumor cells was confirmed by an *in situ* apoptotic assay using Invitrogen's Click-

iT® TUNEL Alexa Fluor® 488 Imaging Assay kit. Cells undergoing apoptosis reveal DNA nicks that the imaging assay kit shows as bright green in color. The images of Fig. 4 show the TC-1 lung carcinoma cells and CL.7 fibroblast cells, treated with Device I, II, and III, 24 h after plasma treatments for 20 s, respectively. The figures show the different effects between TC-1 and CL.7 cells in an identical plasma dose. In the TC-1 cells, most cells are dyed within the plasma treated area. However, in the case of the CL.7 cells, both dyed and un-dyed cells are mixed within the plasma treated area. The TC-1 and CL.7 cells that were treated using the three microplasma jets showed a similar appearance under equivalent plasma treatment time, as is shown in Fig. 4A–F. The presence of both dyed and un-dyed cells indicates that the apoptosis is induced more intensely in TC-1 tumor cells than in CL.7 cells despite the same plasma dosage conditions. That is to say, these assays reveal that mouse lung carcinoma and fibroblast cells have apoptotic selectivity at the same plasma energy. Although the plasma treatment area is larger than the diameter of the hollow-core optical fiber, which is likely due

to the reflection and spread of the reactive species from the plasmas plume volume by the well plate, the results indicate that the microplasma device is able to precisely treat a small collection of tumor cells.

4. Conclusions

Flexible cold microplasma jet devices based on hollow-core glass optical fiber have been proposed for enhanced selective cell targeting. Despite the small inner diameter and the low gas flow rate of the microplasma jet devices, none of the microplasma jets induced necrosis but did induce apoptosis in both cultured mouse lung carcinoma and fibroblast cells. The TC-1 tumor cells were found to be more sensitive to these plasma treatments than murine fibroblast cells under all plasma dose conditions tested. The flexible microplasma jet devices can be employed for microplasma cancer endoscopy and potentially offers a more comfortable therapy method.

Acknowledgments

Appendix A. Supplementary data

Supplementary data associated with this article can be found, in the online version, at doi:10.1016/j.bios.2011.07.039.

References

Becker, K.H., Schoenbach, K.H., Eden, J.G., 2006. J. Phys. D: Appl. Phys. 39, R55–R70.
Cooper, M., Fridman, G., Staack, D., Gutsol, A.F., Vasilets, V.N., Anandan, S., Cho, Y.I., Fridman, A., Tsapin, A., 2009. IEEE Trans. Plasma Sci. 37, 866–871.
Feng, H., Wang, R., Sun, P., Wu, H., Liu, Q., Fang, J., Zhu, W., Li, F., Zhang, J., 2010. Appl. Phys. Lett. 97, 131501.
Fridman, G., Brooks, A.D., Balasubramanian, M., Fridman, A., Gutsol, A., Vasilets, V.N., Ayan, H., Friedman, G., 2007. Plasma Process. Polym. 4, 370–375.
Fridman, G., Shekhter, A.B., Vasilets, V.N., Friedman, G., Gutsol, A., Fridman, A., 2008. Plasma Process. Polym. 5, 503–533.
Georgescu, N., Lupu, A.R., 2010. IEEE Trans. Plasma Sci. 38, 1949–1955.
Hong, Y.C., Uhm, H.S., 2007. Phys. Plasmas 14, 053503.
Jemal, A., Siegel, R., Xu, J., Ward, E., 2010. CA Cancer J. Clin. 60, 277–300.
Jiang, N., Ji, A., Cao, Z., 2009. J. Appl. Phys. 106, 013308.
Karakas, E., Munyanyi, A., Greene, L., Laroussi, M., 2010. Appl. Phys. Lett. 97, 143702.
Kong, M.G., Kroesen, G., Morfill, G., Nosenko, T., Shimizu, T., Dijk, J. van, Zimmermann, J.L., 2009. New J. Phys. 11, 115012.
Kieft, I.E., Broers, J.L.V., Caubet-Hilloutou, V., Slaaf, D.W., Ramaekers, F.C.S., Stoffels, E., 2004. Bioelectromagnetics 25, 362–368.
Kieft, I.E., Kurdi, M., Stoffels, E., 2006. IEEE Trans. Plasma Sci. 34, 1331–1336.
Kim, C.-H., Kwon, S., Bahn, J.H., Lee, K., Jun, S.I., Rack, P.D., Baek, S.J., 2010a. Appl. Phys. Lett. 96, 243701.
Kim, H., Brockhaus, A., Engemann, J., 2009. Appl. Phys. Lett. 95, 211501.
Kim, J., Katsurai, M., Kim, D., Ohsaki, H., 2008. Appl. Phys. Lett. 93, 191505.
Kim, J.-H., Liu, G., Kim, S.H., 2006. J. Mater. Chem. 16, 977–981.
Kim, J.Y., Ballato, J., Foy, P., Hawkins, T., Wei, Y., Li, J., Kim, S.-O., 2010b. Small 6, 1474–1478.
Kim, J.Y., Kim, S.-O., Wei, Y., Li, J., 2010c. Appl. Phys. Lett. 96, 203701.
Kushner, M.J., 2005. J. Phys. D: Appl. Phys. 38, 1633–1643.
Laroussi, M., Lu, X., 2005. Appl. Phys. Lett. 87, 113902.
Lee, H.W., Nam, S.H., Mohamed, A.-A.H., Kim, G.C., Lee, J.K., 2010. Plasma Process. Polym. 7, 274–280.
Lu, X., Xiong, Q., Tang, Z., Jiang, Z., Pan, Y.A., 2008. IEEE Trans. Plasma Sci. 36, 990–991.
Morfill, G.E., Shimizu, T., Steffes, B., Schmidt, H.-U., 2009. New J. Phys. 11, 115019.
Nie, Q.-Y., Ren, C.-S., Wang, D.-Z., Zhang, J.-L., 2008. Appl. Phys. Lett. 93, 011503.
Nikiforov, A.Y., Sarani, A., Leys, C., 2011. Plasma Sources Sci. Technol. 20, 015014.
Noeske, M., Degenhardt, J., Strudthoff, S., Lommatzsch, U., 2004. Int. J. Adhes. Adhes. 24, 171–177.
Rupf, S., Lehmann, A., Hannig, M., Schafer, B., Schubert, A., Feldmann, U., Schindler, A., 2010. J. Med. Microbiol. 59, 206–212.
Sands, B.L., Ganguly, B.N., Tachibana, K., 2008. Appl. Phys. Lett. 92, 151503.
Scholtz, V., Julak, J., Kriha, V., 2010. Plasma Process. Polym. 7, 237–243.
Shashurin, A., Keidar, M., Bronnikov, S., Jurjus, R.A., Stepp, M.A., 2008. Appl. Phys. Lett. 93, 181501.
Somekawa, T., Shirafuji, T., Sakai, O., Tachibana, K., Matsunaga, K., 2005. J. Phys. D: Appl. Phys 38, 1910–1917.
Stoffels, E., Sakiyama, Y., Graves, D.B., 2008. IEEE Trans. Plasma Sci. 36, 1441–1457.
Temmerman, E., Akishev, Y., Trushkin, N., Leys, C., Verschuren, J., 2005. J. Phys. D: Appl. Phys. 38, 505–509.
Tendero, C., Tixier, C., Tristant, P., Desmaison, J., Leprince, P., 2006. Spectrochim. Acta Part B 61, 2–30.
Walsh, J.L., Kong, M.G., 2008. Appl. Phys. Lett. 93, 111501.
Yang, S., Yin, H., 2007. Plasma Chem. Plasma Process. 27, 23–33.